Article

Effect of Cisplatin on Renal Iron Homeostasis Components: Implication in Nephropathy

Ayushi Aggarwal, Amit K. Dinda,* and Chinmay K. Mukhopadhyay*

Read Online

ACCESS | Metrics & More | Article Recommendations | SI Supporting Information

ABSTRACT: Cisplatin is an important chemotherapeutic drug for the treatment of solid tumors but often causes nephropathy as part of the off-target toxicity. Iron accumulation and related damage were implicated in cisplatin-induced kidney injury. However, the role of cisplatin in the renal iron sensing mechanism and its target genes responsible for iron uptake, storage, and release have not been investigated. Cellular iron homeostasis is controlled by the interaction of iron regulatory proteins (IRP1 and IRP2) and iron-responsive elements (IREs) present in the untranslated regions of iron transport and storage components. Here, we report that cisplatin does not influence the expressions of IRP targets such as transferrin receptor-1 (TfR1), divalent metal transporter-1 (DMT1), and ferroportin in renal cells despite the increased heme oxygenase-1 (HO-1) level. Ferritin subunits (Ft-H and Ft-L) are elevated in different magnitudes due to the increased mRNA expression. Intriguingly, a higher expression of Ft-L mRNA is detected than that of Ft-H mRNA. The inability of cisplatin in altering the IRE−IRP interaction is confirmed by examining IRE-containing luciferase activity, RNA electrophoretic mobility shift assay, and activation of IRPs. The labile iron pool is depleted but reversed by silencing of either Ft-H or Ft-L, suggesting increased iron storage by ferritin. Silencing of Ft-H or Ft-L promotes cell death, suggesting that ferritin acts to protect the renal cells from cisplatin-mediated toxicity. A differential increase of transcripts and equivalent increase of proteins of Ft-H and Ft-L and unaltered TfR1 and DMT1 transcripts are found in the kidneys of cisplatin-treated rats along with iron accumulation. Our results reveal that cisplatin does not influence the IRE−IRP interaction despite alteration of the cellular iron pool in renal cells. This insensitivity of the IRE−IRP system may be implicated in the accumulation of iron to contribute to cisplatin-induced nephropathy.
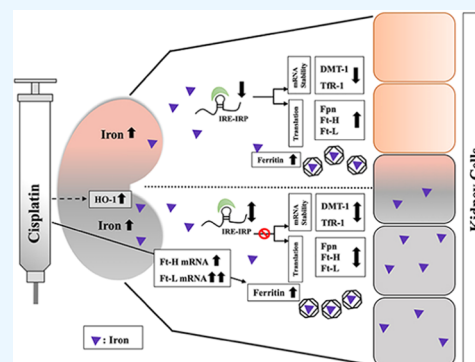
1. INTRODUCTION

Cisplatin is one of the most widely used chemotherapeutic drugs to treat solid tumors including ovarian, head and neck, and testicular germ cell tumors. It causes several off-target toxicities including ototoxicity, gastrointestinal toxicity, myelosuppression, and allergic reactions;[1,2] however, the main dose-limiting side effect of cisplatin is nephrotoxicity.[3,4] Studies in recent years revealed that cisplatin might be transported and accumulated into renal cells by copper transporter Ctr1[5] and organic cationic transporter OCT2 (SLC22A2).[6,7] Several mechanisms are attributed to cisplatin-induced nephrotoxicity including biotransformation to more potent toxins,[8] by forming adducts with DNA, RNA, and proteins.[9] Evidence of cisplatin-induced mitochondrial DNA damage has also been provided.[10] It may cause apoptosis in relatively lower concentrations, while higher concentrations may result in necrosis.[8] The role of TNFα in cisplatin-induced renal injury has also been substantiated.[11] Evidence from several studies also provided data about a critical role of catalytic iron in cisplatin-induced nephrotoxicity,[12,13] and iron chelators are found to ameliorate the cisplatin-induced nephrotoxicity,[12] suggesting that cisplatin may have a direct influence on iron metabolism in renal cells.

Kidney is rich in mitochondria containing heme iron and iron−sulfur proteins critical for electron transport chain function.[14] Iron is filtered in the glomerulus and reabsorbed in the renal tubules.[15,16] Renal cells can absorb both transferrin-bound iron (TBI) and non-transferrin-bound iron (NTBI). TBI is taken up by the transferrin receptor-1 (TfR1). ZIP8 and ZIP14 are expressed in proximal tubules and can transport NTBI, cadmium, and manganese.[17] Even L-ferritin-bound iron can be taken up by binding with Scara5, a protein expressed in the kidney stroma.[18,19] Along the length of the nephron, iron may be absorbed by DMT1, ZIP8, and ZIP14.[20,21] DMT1 is expressed in the cortex and not in the medulla and is present at the brush border and apical pole of epithelial cells of proximal tubules.[14] An increase in iron uptake enhances the labile iron pool (LIP). Iron may be distributed from the LIP to different
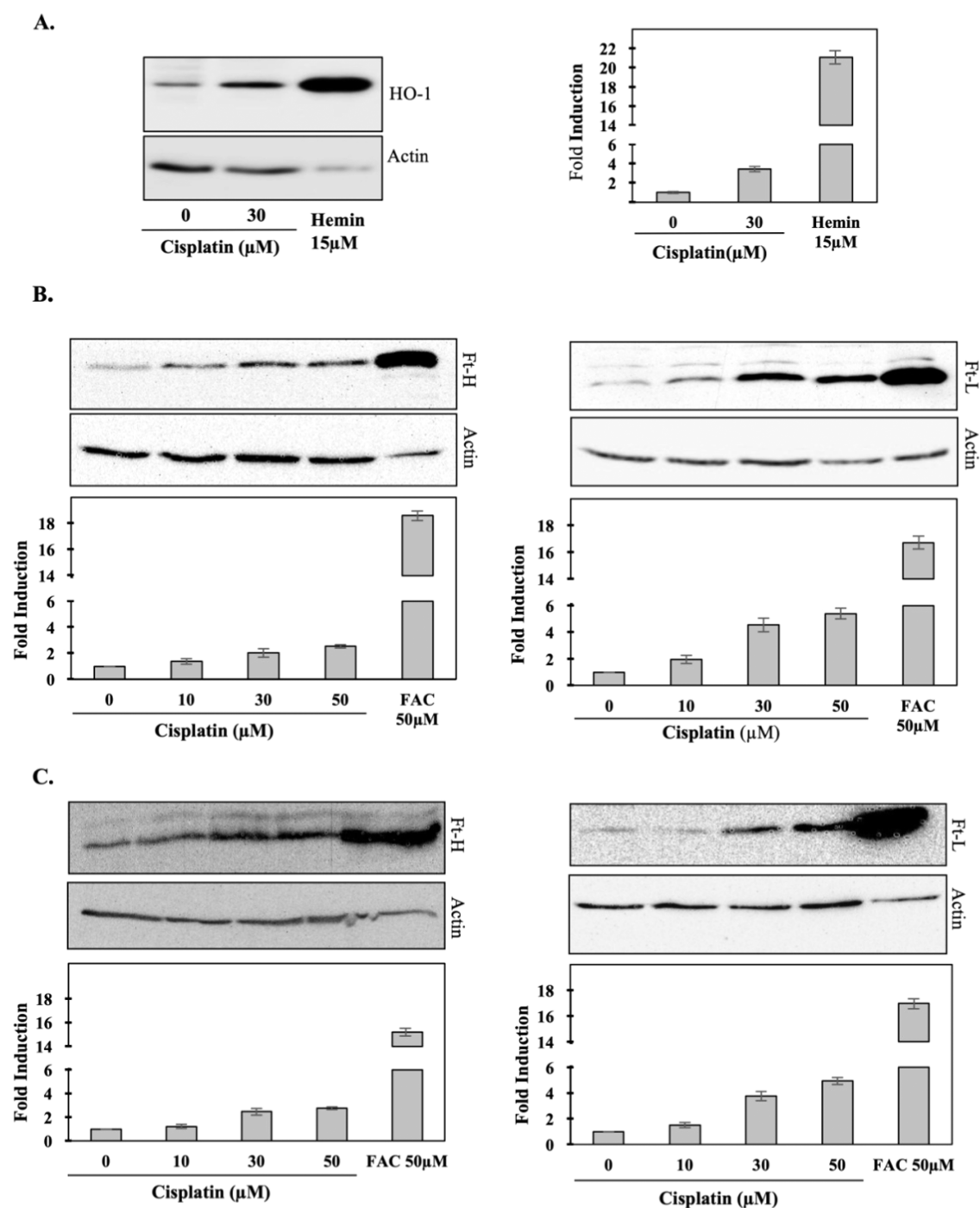
Figure 1. Effect of cisplatin on heme oxygenase-1 and ferritin in renal cell lines. (A) HEK-293 cells were treated with cisplatin (0 and 30 μM) for 16 h, and the HO-1 level was detected by western blot analysis in whole cell lysate. Hemin (15 μM) was used as a positive control, but a less amount of lysate (20 μg) was loaded. The right panel represents densitometric analysis from three independent experiments. Ferritin (H, left panels and L, right panels) protein levels were detected in whole cell lysates of HEK-293 (B) and HK-2 (C) cells treated with cisplatin (0−50 μM) for 16 h. FAC (50 μM) was used as a positive control. Densitometric quantifications were performed from at least three independent experiments and presented in the lower panel (B, C). Data represented as mean ± SD.

cellular destinations or may be stored into ferritin for future needs and to avoid iron-induced toxicity. Ferritin is composed of two subunits (H and L) and can store up to 4500 iron atoms. Ferritin-H (Ft-H) contains ferroxidase (Fe^{2+} to Fe^{3+}) activity that helps to store iron in the mineral core, while ferritin-L (Ft-L) facilitates nucleation and mineralization of the iron center.[22] Excess iron is released by ferroportin (Fpn), which is the unique iron exporter for all mammalian cells.[23] Despite being an

essential nutrient, iron is highly toxic particularly in the presence of reactive oxygen species (ROS) due to its redox-active nature. Thus, iron homeostasis is intricately regulated mostly by post-transcriptional mechanisms.[24] The cellular iron level is sensed by iron regulatory proteins (IRP1 and IRP2). During iron depletion, cytosolic aconitase IRP1 transforms into an RNA-binding form to bind iron-responsive elements (IREs) present in 3′untranslated regions (3′UTRs) of TfR1 and DMT1 to
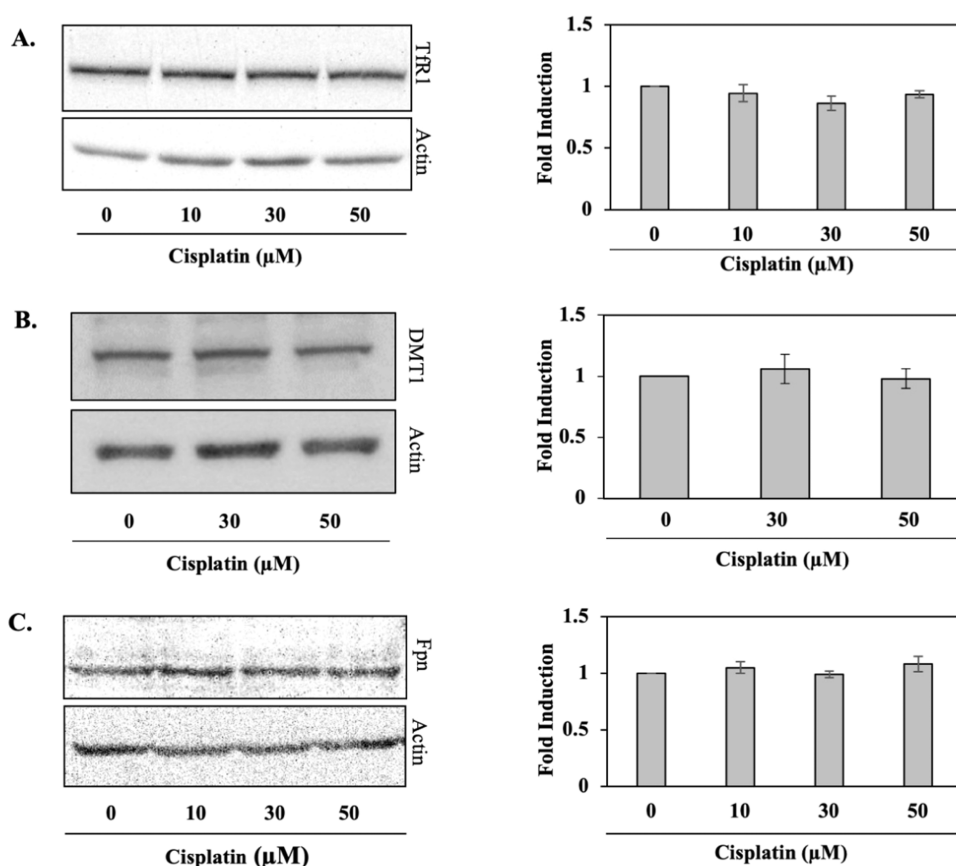
Figure 2. Effect of cisplatin on the expression of TfR1, DMT1, and ferroportin. HEK-293 cells were treated with cisplatin ($0-50\ \mu M$) for 16 h, and cell lysates were subjected to immunoblot analysis for TfR1 (A), DMT1 (B), and ferroportin (C). Actin was used for loading the control. The left panel shows immunoblots, and the respective right panel shows densitometry analysis representing mean $\pm$ SD from three independent experiments.

promote the stability of their transcripts for enhancing iron uptake. At the same time, IRP1 can bind 5′UTRs of ferritin subunits and ferroportin to block their translation so that iron can be utilized for essential cellular functions. IRP2 is regulated by the post-translational protein stability mechanism inversely with the cellular iron content and functions similarly like IRP1 by binding to IREs present in the UTRs of the respective iron homeostasis components to control their abundance.[24,25] When the iron level is excess, IRP1 converts into cytosolic aconitase and IRP2 is destabilized so that ferritin translation is enhanced to store iron and ferroportin translation is increased to release iron. At the same time, TfR1 and DMT1 mRNAs are decreased due to the affected IRE−IRP interactions in their UTRs, resulting in less iron uptake.[24]

Like redox-active iron, heme iron also can exert toxic effects on the kidney and has been known to induce acute kidney injury (AKI).[14] Renal cells could be protected against heme-induced toxicity by upregulating heme oxygenase-1 (HO-1) that would degrade heme to biliverdin and ferrous iron to trigger the generation of cytoprotective carbon monoxide and Ft-H.[26] HO-1 also modulates oxidative stress by producing antioxidant biliverdin and bilirubin by breaking down heme.[27] Incidentally, HO-1 is reported to be increased to protect against the nephrotoxicity of cisplatin;[28] however, this would lead to an increase in the free catalytic iron. This free iron should influence the IRE−IRP system to alter renal iron homeostasis. Interestingly, it has recently been reported that cisplatin inactivates the IRE−IRP system by binding with IRP2,[29] resulting in increased ferritin-H translation and simultaneously

decreased TfR1 and DMT1 in human colon adenocarcinoma cells and several other human cell types (HeLa, MCF7, K562). However, the role of cisplatin in the IRE−IRP system and its target components in renal cells have not been investigated so far. In this study, we addressed this issue in multiple renal cells and in the kidneys of cisplatin-injected rats. Our results reveal that cisplatin does not alter any IRE−IRP targets such as TfR1, DMT1, or Fpn. It also does not influence the activity of IRE-containing 5′ UTRs of Ft-H or Ft-L but alters the mRNA expression of ferritin subunits. The unaltered IRE−IRP response despite a strong increase in HO-1 by cisplatin may lead to iron accumulation and subsequent nephropathy.

2. RESULTS

2.1. Cisplatin Upregulates HO-I and Iron Storage Protein Ferritin in Renal Cell Lines. Cisplatin is reported earlier to induce HO-1 in renal cells.[28] Therefore, we initially tested the HO-1 expression in the presence of cisplatin ($30\ \mu M$, 16 h). We observed more than threefold increase in the HO-1 protein level detected by western blot analysis in HEK-293 cells (Figure 1A). Hemin was used as a positive control. Since HO-1 can degrade heme to release iron, we hypothesized that the released iron might increase ferritin synthesis. We detected a concentration-dependent increase in the Ft-H protein level by cisplatin treatment ($0-50\ \mu M$) in HEK-293 cells. The Ft-H protein expression was increased more than twofold by cisplatin ($50\ \mu M$) treatment (Figure 1B, left panel). However, the Ft-L protein expression was found to be more than fivefold higher with cisplatin ($50\ \mu M$) treatment (Figure 1B, right panel).
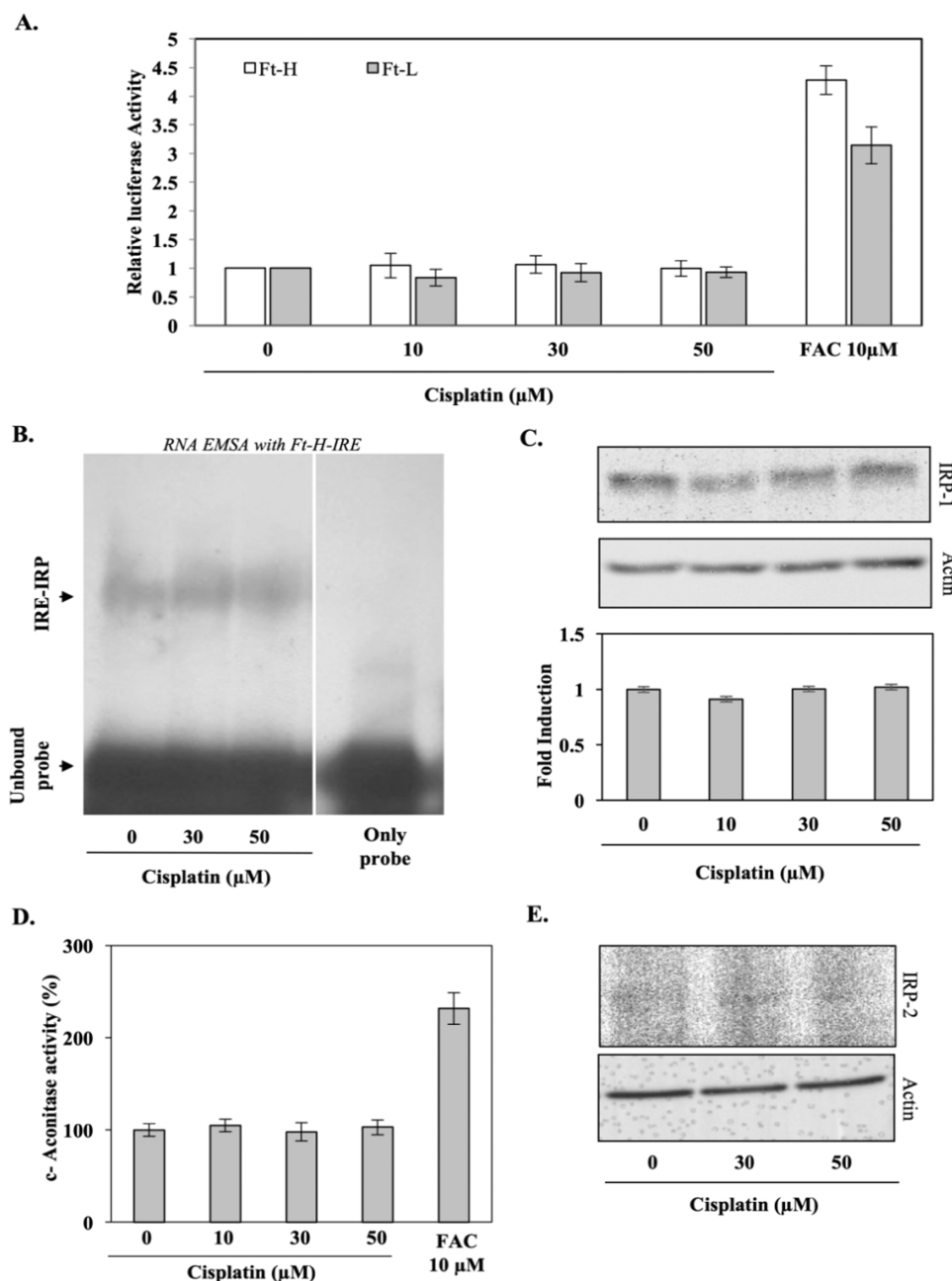
Figure 3. Effect of cisplatin on the IRE−IRP system. (A) Ft-H-IRE- and Ft-L-IRE-containing plasmids were transfected separately in HEK-293 cells and treated with cisplatin (0−50 μM) for 16 h. Relative luciferase activity was measured in cell lysates by dual-luciferase assay. Renilla luciferase was used as a transfection control. Results represented from three independent experiments performed in triplicate. Iron salt FAC (10 μM) was used as a positive control. (B) IRE−IRP interaction was verified by RNA-EMSA using ^{32}P-labeled Ft-H 5′UTR and cytosolic extract from cisplatin-treated (0−50 μM) HEK-293 cells for 12 h. Only the probe was shown on the rightmost lane. The result represents one of the three independent experiments. (C) IRP1 western blot analysis was performed in cytosolic extracts (60 μg) isolated from cisplatin-treated (0−50 μM, 16 h) HEK-293 cells. Actin was used as a loading control. The bottom panel shows densitometric analysis from three independent experiments. (D) Aconitase activity assay was performed from cytosolic extracts isolated from cisplatin-treated (0−50 μM, 16 h) HEK-293 cells. FAC (10 μM) was used as a positive control. E. Western blot analysis for IRP2 was performed using cytosolic extracts (100 μg) from cisplatin-treated (0−50 μM, 16 h) HEK-293 cells. The blot represents one of the three independent experiments. Actin was used as a loading control. Due to the unclear IRP2 signal, no quantification was performed. The bar graph represents mean ± SD.

Cisplatin-related renal damage was shown to target the proximal tubular epithelial cells of the kidneys.[30] Therefore, we further tested the effect of cisplatin on the ferritin protein level in the proximal tubular epithelial cell line HK-2. We detected similar results by western blot analyses (Figure 1C) as Ft-H was induced more than twofold (left panel), while Ft-L was increased by about fivefold (right panel) by cisplatin (50 μM)

treatment. These results suggest that cisplatin regulates ferritin subunits differentially in renal cells.

2.2. Cisplatin Does Not Alter TfR1, DMT1, and Fpn in Renal Cells. We further examined the effect of cisplatin on other iron homeostasis components such as TfR1, DMT1, and Fpn; these are targets of the IRE−IRP system. Cisplatin treatment (0−50 μM, 16 h) did not show any change in iron
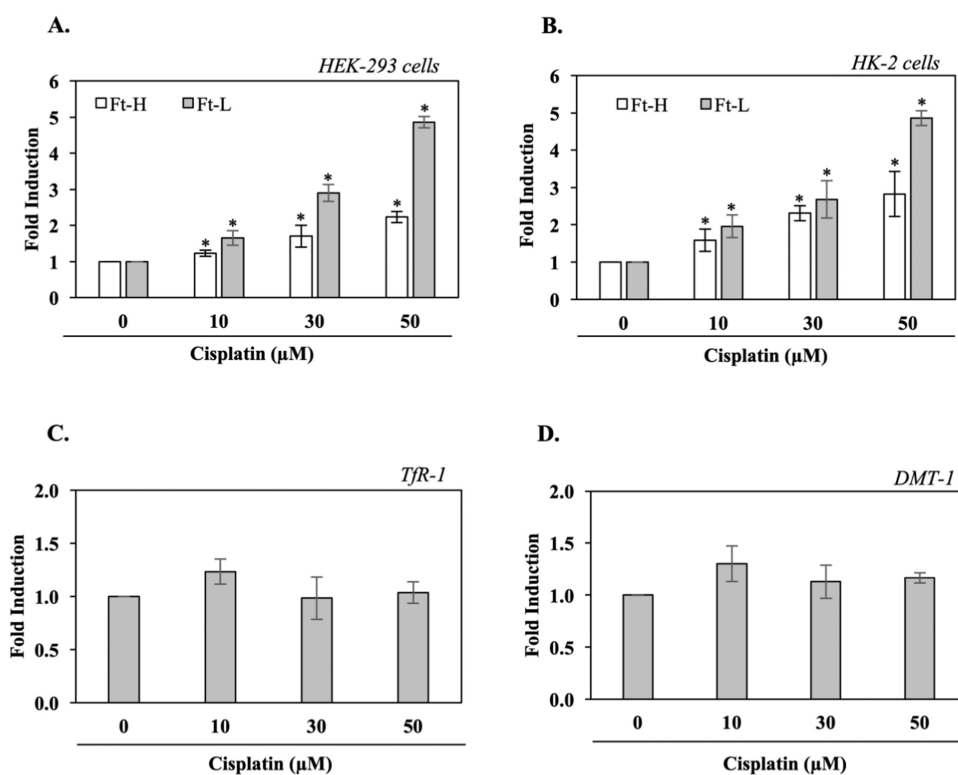
Figure 4. Effect of cisplatin on the transcripts of ferritin subunits, TfR-1 and DMT-1. HEK-293 (A) and HK-2 (B) cells were treated with cisplatin (0−50 μM) for 16 h, and Ft-H and Ft-L mRNA expressions were determined by qRT-PCR analysis. Similarly, TfR1 (C) and DMT1 (D) mRNA expressions were determined by qRT-PCR analysis from cisplatin (0−50 μM)-treated HEK-293 cells for 16 h. In all cases, β-actin was used for normalization (*p value < 0.05).

uptake components, TfR1 and DMT1 protein levels, in HEK-293 cells (Figure 2A,B). Similar treatment of cisplatin also did not alter the iron exporter protein Fpn (Figure 2C). We also observed unaltered TfR1, DMT1, and Fpn expressions in HK-2 cells (data not shown). These results suggest that cisplatin has no effect on the iron uptake and iron release capacity in renal cell types despite altering HO-1 and ferritin levels.

2.3. Cisplatin Does Not Modulate the IRE−IRP Interaction but Augments the mRNA Expression of Ferritin Subunits. Since cisplatin-induced HO-1 might release iron from heme, one of the possibilities of the ferritin induction could be modulation of the IRE−IRP interaction to increase the translation of both subunits. To verify that we have transfected HEK-293 cells with Ft-H-IRE- or Ft-L-IRE-containing luciferase constructs prior to the cisplatin (0−50 μM, 16 h) treatment. Results showed no alteration in luciferase activity by cisplatin treatment (Figure 3A); however, only FAC (iron salt) treatment induced luciferase activity for both Ft-H-IRE and Ft-L-IRE between three- and fourfold (Figure 3A). These results suggest that cisplatin-induced ferritin regulation may not be mediated by the IRE−IRP interaction. To find the effect of cisplatin on the IRE−IRP interaction, we performed RNA electrophoretic mobility shift assay (EMSA) using a radiolabeled Ft-H-IRE probe, and no altered interaction was observed (Figure 3B). Furthermore, we examined the expressions of cellular iron sensors IRP1 and IRP2. IRP1 having aconitase activity is regulated by a post-translational mechanism,[25] while IRP2 is stabilized by iron depletion.[31] We did not find any change in the IRP1 protein level and cytosolic aconitase activity by cisplatin treatment (Figure 3C,D). As expected, iron salt (FAC, 10 μM) treatment substantially increased the cytosolic aconitase activity

(Figure 3D). We did not find any appreciable signal/alteration of IRP2 in cisplatin-treated HEK-293 cells (Figure 3E), a similar observation reported earlier.[29] However, the same antibody was more effective in detecting IRP2 protein abundance in other cell types (Figure S1). These results suggest that cisplatin does not influence the IRE−IRP interaction and the presence of negligible abundance of IRP2 in renal cells. Thus, to understand the mechanism of ferritin regulation, we tested the expressions of Ft-H and Ft-L mRNAs in cisplatin-treated renal cell lines. We detected increased Ft-H and Ft-L mRNA levels in both HEK-293 (Figure 4A) and HK-2 cells (Figure 4B). Interestingly, like protein levels, we found a higher increase in Ft-L mRNA than Ft-H mRNA in both cell lines. Cisplatin treatment did not alter TfR1 and DMT1 transcript levels in HEK-293 cells (Figure 4C,D) and in HK-2 cells (data not shown).

Since both TfR1 and DMT1 contain IREs in the 3′UTR and these IREs are known to provide stability in their transcripts,[24] no alteration of TfR1 and DMT1 mRNAs further suggests that cisplatin does not influence the IRE−IRP interaction in renal cell types.

2.4. Cisplatin Regulates Ferritin Subunits in 786-O Renal Cancer Cells by Augmenting the mRNA Expression. A recent report had shown that cisplatin could regulate ferritin by binding directly with the iron sensor protein IRP2 to enhance the translation of ferritin in adenocarcinoma cells,[29] whereas we detected an increased ferritin expression that could be due to an increase in mRNA of the subunits in renal cell lines. This difference could be due to that Miyazawa et al.[29] considered cancer cells for their study. Therefore, we wanted to investigate the effect of cisplatin on 786-O renal adenocarcinoma cells. Cells were treated with increasing concentration (0−50 μM) of
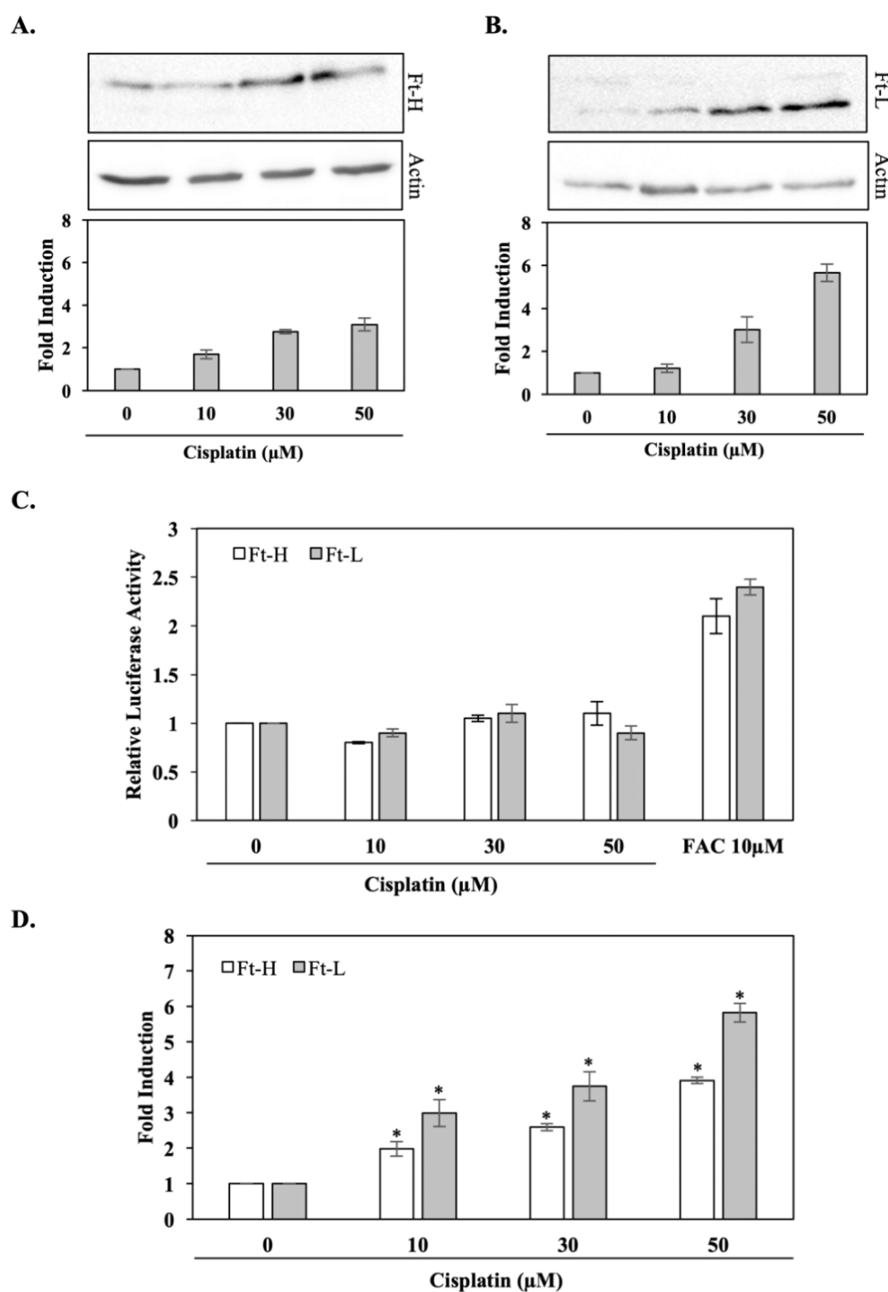
Figure 5. Effect of cisplatin on the ferritin expression in renal adenocarcinoma 786-O cells. Cells were treated with cisplatin (0−50 μM) for 16 h. Total cell lysates were subjected to immunoblot analyses for Ft-H (A) and Ft-L (B). Actin was used as a loading control. The bottom panel represents the relative expressions of Ft-H and Ft-L from three independent experiments. (C) Ft-H-IRE- and Ft-L-IRE-containing plasmids were transfected separately along with the renilla luciferase-containing plasmid, and then, cells were treated with cisplatin (0−50 μM) for 16 h. Relative luciferase activity was measured in cell lysates by dual-luciferase assay. Results represented from three independent experiments performed in triplicate. Iron salt FAC (10 μM) was used as a positive control. (D) Ft-H and Ft-L mRNA expressions were determined by qRT-PCR after cisplatin (0−50 μM) treatment for 16 h. The bar graph represents mean ± SD (*p value < 0.05).

cisplatin for 16 h, and then, western blot analyses were performed for Ft-H and Ft-L. Results showed that cisplatin could regulate Ft-H and Ft-L proteins about three- and sixfold, respectively, like other renal cell lines (Figure 5A). Cisplatin did not show any effect on the IRE−IRP interaction as detected by luciferase assay (Figure 5B) unlike other adenocarcinoma cells.[29] Furthermore, cisplatin induced a higher expression of Ft-L mRNA than Ft-H mRNA like other renal cell lines (Figure 5C). These results reveal that cisplatin regulates the transcripts of ferritin subunits differentially in renal cells.

2.5. Cisplatin-Induced Ferritin Could Store Iron to Protect Cells from Toxicity.

An earlier report[28] and our observation (Figure 1A) showed that cisplatin could induce HO-1 to release heme-bound iron with a simultaneous increase in ROS (Figure S2) that together could affect cell viability. We assumed that an increased ferritin expression would store the iron from the labile iron pool (LIP) to avoid cellular damage. To test this assumption, we initially silenced ferritin subunits individually and estimated LIP using calcein-AM, a widely adopted fluorescent probe for monitoring iron levels.[32,33] Green fluorescence derived from calcein in cells is inversely related with

the LIP as the fluorescence is quenched upon binding to intracellular iron.

We detected about 60% decreases of ferritin subunits in HK-2 cells (Figure 6A) and in HEK-293 cells (data not shown) by transfecting specific siRNAs. A concentration-dependent increase in calcein-sensitive fluorescence was detected by cisplatin (0−50 μM) treatment in control siRNA-transfected cells (Figure 6B, first three panels); these were partially reversed in FT-H-or Ft-L-silenced HEK-293 and HK-2 cells (Figure 6B). A quantitative determination showed Ft-L or Ft-H silencing reversed about 60% of the LIP level than in control siRNA-transfected HK-2 cells (Figure 6C). Iron chelator DFO was used as a positive control for LIP assay. These results clearly show the ability of cisplatin-induced ferritin in storing iron from the LIP. An earlier study reported a significant increase in apoptosis in cisplatin-challenged proximal tubule-specific Ft-H knockout mice, suggesting a protective role of Ft-H.[30] Therefore, we have performed apoptotic cell death assay to test the hypothesis that an increase in the ferritin level was to protect the kidney cells from cisplatin-induced toxicity. Transfection with Ft-H or Ft-L siRNA showed a significant increase in apoptotic cells compared with the control siRNA-transfected cells as determined by double staining of Annexin-V and PI (Figure 6D). H_2O_2 (50 μM) was used as a positive control for apoptotic cell death. Survival of HK-2 cells was found to be about 82% by control siRNA transfection, about 43% in Ft-L siRNA, and about 45% in Ft-H siRNA-transfected cells after cisplatin treatment (50 μM, 24 h) (Figure 6E). These results suggest a protective role of ferritin against cisplatin-induced toxicity in renal cells.

2.6. Cisplatin Promotes Ferritin Subunits and Iron Accumulation in the Rat Kidney. To find the effect of cisplatin on ferritin expression in vivo, we have adopted an animal model by injecting cisplatin into male Wistar rats ($n = 6$), as depicted in Figure 7A. Rats were injected with cisplatin (1 mg/kg body weight) or saline (vehicle) twice a week up to 8 weeks. We adopted this model of chronically injecting cisplatin to resemble a patient treatment module. To confirm that cisplatin was effective in promoting kidney damage, we tested the serum creatinine level and assessed the histopathology of kidney parenchyma by MT and PAS staining. Results showed a time-dependent increase in the serum creatinine level in cisplatin-injected animals compared to that in saline-injected animals (Figure 7B). We also found increased serum ferritin in cisplatin-injected rats (Figure S3) as reported earlier.[30] Renal histology also corroborated the cisplatin-induced kidney injury by damage of tubular epithelial cells with the appearance of tubular casts and interstitial fibrosis and deposition of collagen as detected by MT staining in the cisplatin-injected rat kidneys (Figure 7C, upper panels). Similarly, PAS staining showed increased vacuolization and loss of the brush border membrane of tubular epithelial cells with focal denudation in cisplatin-treated rat kidneys (Figure 7C, lower panels). A substantial increase in the tubular damage score and tubulointerstitial fibrosis score was found in cisplatin-treated rat kidneys compared to vehicle-treated animals (Figure 7D). After confirming cisplatin-induced kidney damage in rats, we then examined the mRNA levels of Ft-H and Ft-L in kidney tissue by qRTPCR analysis. A higher increase in Ft-L mRNA than Ft-H mRNA was detected in renal cell lines in cisplatin-injected rats (Figure 8A). However, there were no significant alterations of TfR1 and DMT1 transcript levels (Figure 8B), suggesting that IRE−IRP interactions remained unaltered. Furthermore, we
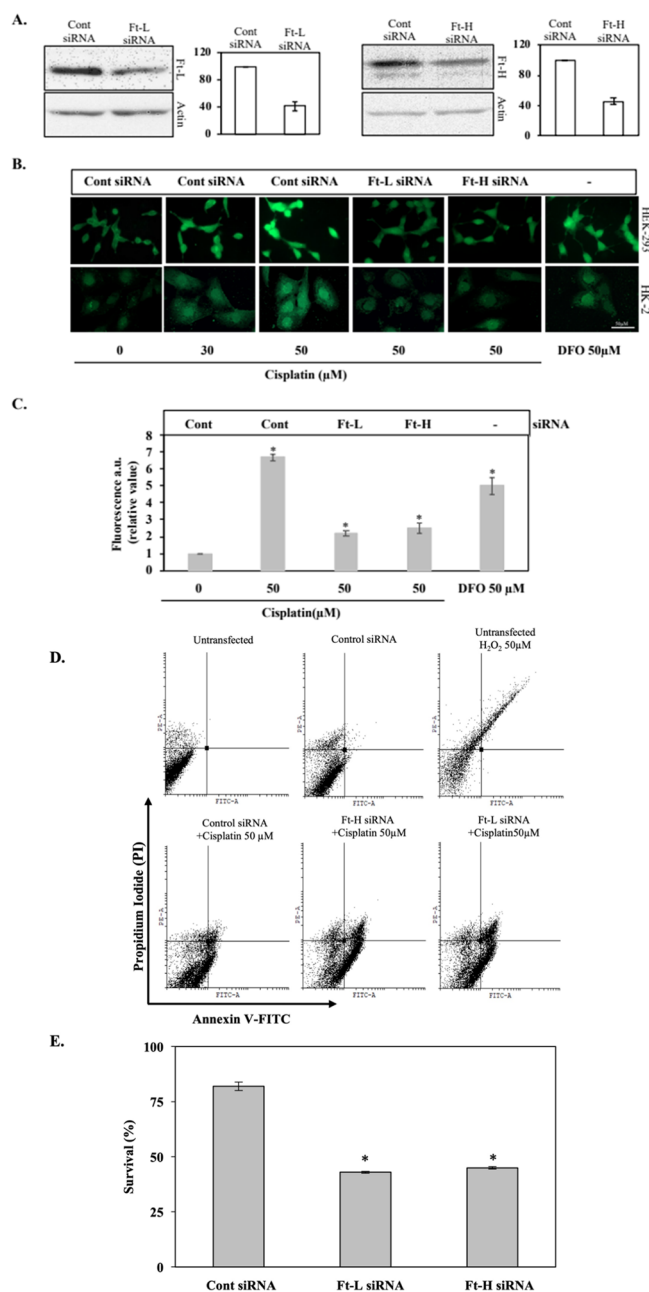

Figure 6. Ferritin stores the labile iron pool and protects cells from cisplatin-induced toxicity. (A) Ft-H and Ft-L were silenced using specific siRNA as shown by immunoblot in HK-2 cells. (B) LIP levels were determined by calcein-sensitive fluorescence detected by microscopy in HEK-293 (upper panels) and HK-2 cells (bottom panels). The first three panels from left represent control siRNA-transfected cells treated with cisplatin (0−50 μM). The fourth and fifth panels represent Ft-L- and Ft-H-silenced cells, respectively, treated with cisplatin (50 μM). The sixth panel represents iron chelator DFO-treated cells as a positive control. (C) LIP was estimated in HK-2 cells by calcein-AM assay under similar conditions as described in B. Results represent mean ± S.D. from three independent experiments. (D) Cisplatin-induced apoptosis was examined by Annexin V/propidium iodide staining using FACS in HK-2 cells. E. The bar graph represents mean % survival of HK-2 cells from three independent experiments. The error bar shows SD (*p value < 0.05).

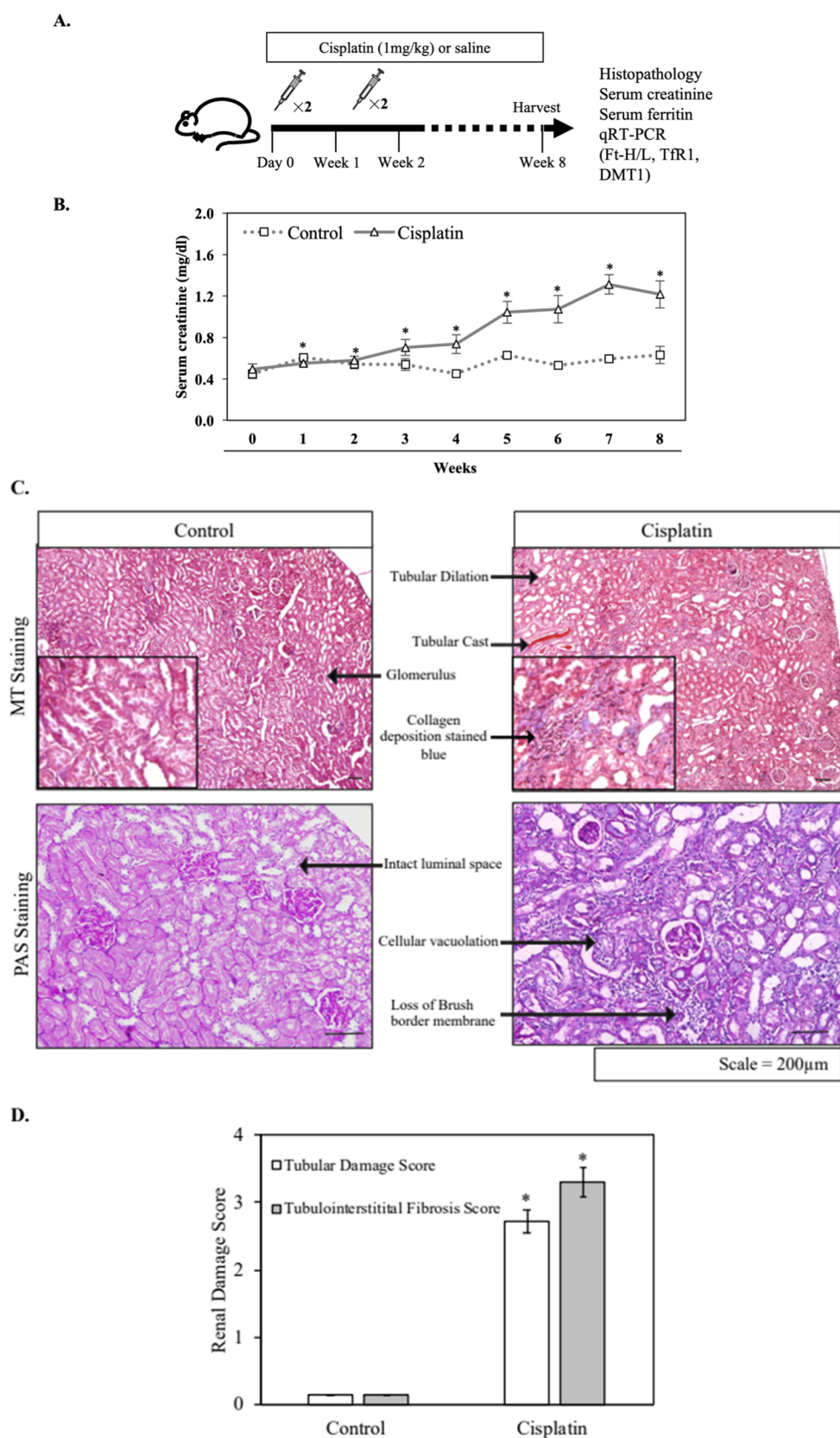examined Ft-H and Ft-L protein expression by western blot analysis.

Figure 7. Cisplatin promotes kidney tissue injury in Wistar rats. (A) Schematic diagram of the cisplatin or saline treatment protocol in male Wistar rats. (B) Weekly serum creatinine levels (0−8 weeks) of cisplatin-treated and vehicle-injected rats ($n = 6$). Results represent mean ± SD. (*p value < 0.05). (C) Histological determination of kidney damage by MT staining (upper panels) and PAS staining (lower panels) between the vehicle- and cisplatin-injected rats. Scale bar: 200 μm. The inset is a magnified portion from the same image. (D) Bar graph shows the tubular damage score and tubulointerstitial fibrosis score. Mean values were calculated from observing 10 nonoverlapping regions from each animal ($n = 6$), error bars representing SD (*p value < 0.05).
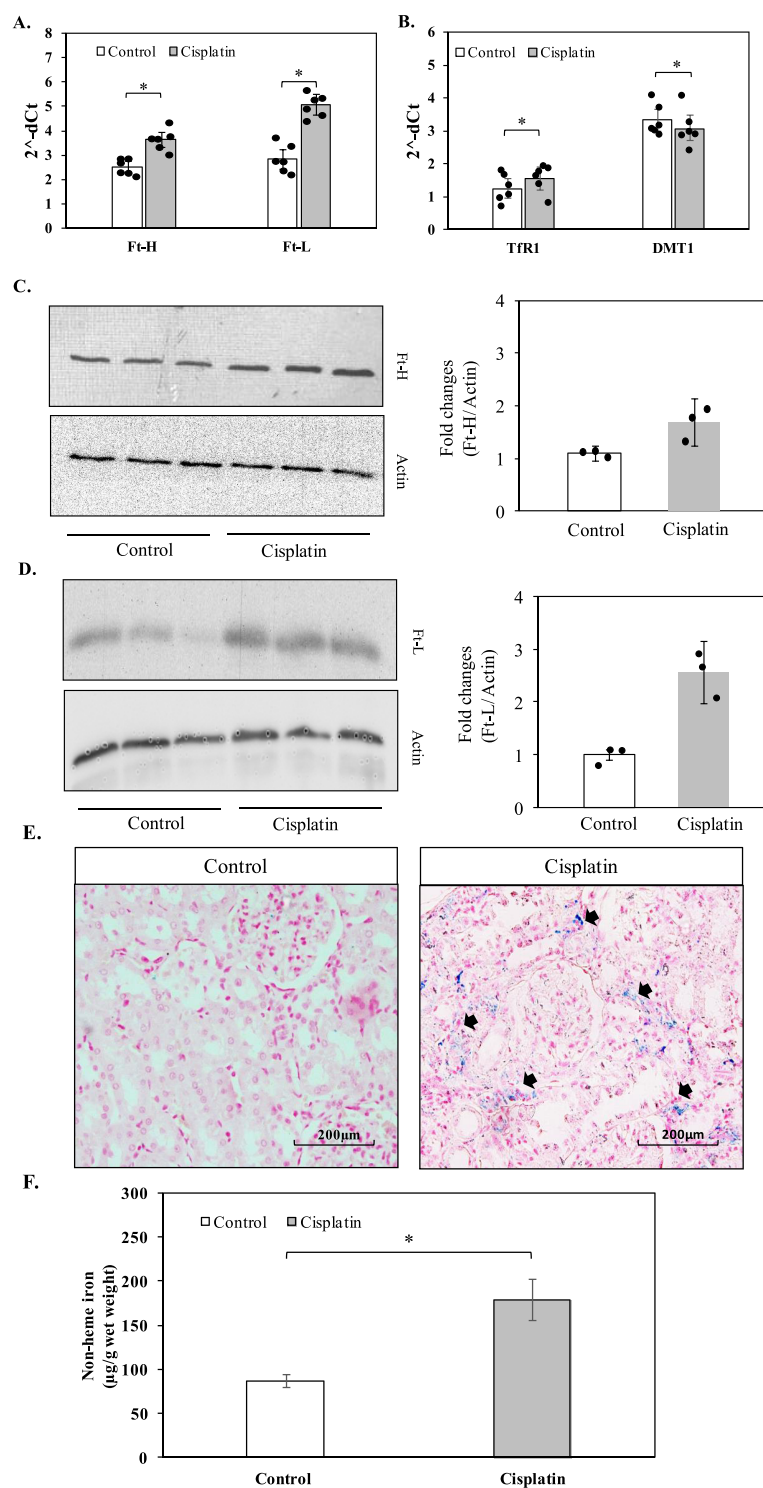
Figure 8. Effect of cisplatin on ferritin and iron levels in the kidney of Wistar rats. (A) Ft-H and Ft-L mRNA expressions were determined in kidney tissues of vehicle (control)- vs cisplatin-injected rats by qRT-PCR ($n = 6$). B. Expressions of TfR1 and DMT1 mRNA expressions in kidney tissues of vehicle (control)- vs cisplatin-injected rats by qRT-PCR ($n = 6$). (C) Western blot analysis for Ft-H and Actin was performed for vehicle (control)- and cisplatin-injected kidney tissues ($n = 3$). (D) Similarly, Ft-L and actin western blot was performed in vehicle (control)- and cisplatin-injected kidney tissues ($n = 3$). Quantitation was shown for both in right panels. (E) Perl's Prussian blue staining of kidney sections from control and cisplatin-injected Wistar rats. The black arrows indicate iron deposition. (F) Non-heme iron estimation in kidney tissue lysates represented as μg of iron per gram of wet tissue weight. The bar graph indicates mean $\pm$ SD calculated from animals of each group ($n = 6$) (*p value < 0.05).

Results showed an increased level of Ft-H (Figure 8C) and Ft-L (Figure 8D) in the kidneys of cisplatin-treated rats compared to that in vehicle-treated control rats. Intriguingly, the protein level of Ft-H was increased less than that of Ft-L like mRNA

levels (Figure 8A). We detected iron accumulation by Perl's staining (Figure 8E) and about a twofold increase in non-heme iron in the cisplatin-injected kidneys (Figure 8F). These results show that cisplatin treatment alters the mRNA and protein

expression of ferritin subunits differentially but does not influence IRE-IRP targets despite significant accumulation of the renal iron pool.

3. DISCUSSION

Cisplatin has long been employed for chemotherapy of cancer patients diagnosed with solid tumors. It also causes cytotoxicity in noncancer cells, causing deleterious effects in various vital organs particularly in the kidneys. Cisplatin promotes iron accumulation in the kidneys[12,13] and is well known to generate higher ROS[34] (Figure S2). ROS in conjunction with accumulated iron may damage kidney tissue. However, the influence of cisplatin on kidney iron homeostasis particularly in the IRE-IRP system is poorly understood so far. The current study revealed that cisplatin could increase Ft-H and Ft-L levels by promoting the respective mRNA expression in renal cell types and in rat kidney but did not show any effect on TfR1, DMT1, and ferroportin. These results strongly suggest that during cisplatin treatment, iron-sensing machinery mediated by the IRE–IRP interaction remains unaltered despite a strong increase in the HO-1 expression, which is known to release iron by heme degradation. We also detected that an increased ferritin level could protect cells from cisplatin-induced toxicity by storing iron. Our findings thus may help in understanding kidney iron accumulation in cisplatin-treated kidney tissue.

Intriguingly, it has been recently reported that cisplatin could form a complex with the iron sensor IRP2 to influence the IRE–IRP interaction, resulting in increased ferritin translation and decreased TfR1 and DMT1 expressions by affecting mRNA stability in several cancer cell types.[29] This results in less iron availability for cell proliferation and provides a novel mechanism of the anticancerous effect of cisplatin. However, our data clearly show that the IRE–IRP interaction remains unaltered in multiple renal cells. Similarly, we found that the expressions of IRE-containing transcripts such as TfR1 and DMT1 remained unaltered in the kidneys, suggesting unresponsiveness of the IRE–IRP system by cisplatin treatment. Interestingly, we did not detect any influence on the IRE–IRP system in the renal carcinoma cell line 786-O, but cisplatin could induce Ft-H and Ft-L transcripts and proteins (Figure 4). All these results suggest that cisplatin can influence iron homeostasis in kidney cells differently from various cancer cells reported in the previous study.[29] This difference in the effect of cisplatin on iron homeostasis may be attributed to differential expressions of IRP1 and IRP2 in kidney cells from other cell types. It is well documented that the kidney has the highest expression of IRP1 compared to various other tissues.[14] Animals lacking IRP1 are unable to repress ferritin synthesis fully in the kidney during iron deficiency, implying that mainly, IRP1 contributes to the regulation of iron metabolism in the kidney,[14,16] whereas in general, IRP2 is over-expressed in different cancer cells and plays a critical role in tumor growths.[35−37] Thus, the ability of cisplatin in forming a complex mainly with IRP2 in altering IRE–IRP targets in different cancer cells may not be effective in renal cells due to the negligible abundance of IRP2. It is to be noted that IRP2 could not be detected in HEK293 cells in an earlier report,[29] while we could detect only a negligible amount (Figure 3), although the same antibody was useful in detecting IRP2 in different cell types (Figure S1) as we reported earlier.[38−40]

We detected Ft-H and Ft-L mRNA regulation in both cisplatin-treated rat kidneys and in three different renal cell lines. Interestingly, in all of these instances, Ft-L mRNA is regulated more than Ft-H mRNA. In cisplatin-treated renal cell lines and

rat kidneys, a higher increase of the Ft-L protein was detected than Ft-H by western blot analysis, suggesting that differential regulation of mRNAs was responsible for the differential increase in protein levels. Ft-H contains ferroxidase activity and contributes to iron loading into ferritin, while Ft-L is involved in the nucleation of iron.[22,24] We detected a dose-dependent depletion of LIP by cisplatin in both HEK293 and HK-2 cells (Figure 6). Silencing of either Ft-H or Ft-L reversed the LIP in both cell types, confirming the storing of iron into ferritin. Otherwise, the increased cellular iron level potentially could damage renal cells in conjunction with cisplatin-induced ROS generation[34] (Figure S2). An earlier study revealed the role of Ft-H in proximal tubule-specific knockout mice in protecting cells from cisplatin-induced acute kidney injury.[30] An increased apoptosis was detected in these mice in proximal tubular cells by glycerol or cisplatin treatment. This finding supports our observation of increased apoptotic cell death in Ft-H/Ft-L-silenced proximal tubular HK-2 cells. Thus, our data and the previous finding strongly suggest that the cisplatin-induced increased ferritin level plays a protective role against cisplatin-induced iron accumulation and related kidney damage.

In this study, we have adopted a model of cisplatin-induced nephropathy in rats to resemble the treatment of patients. Cisplatin was injected in chronic doses (1 mg/kg body weight twice a week) over a period of 8 weeks. The nephropathy was confirmed with histopathological observation and increased serum creatinine levels. Importantly, we detected a substantial iron accumulation in kidney tissue by Perl's staining and non-heme iron estimation. As reported earlier, we also detected increased serum ferritin in cisplatin-treated rats.[30] Interestingly, despite the higher iron accumulation, we did not find any alteration of IRE-containing transcripts such as TfR1 and DMT1 in the kidneys, but a higher level of increased Ft-L mRNA was detected than Ft-H mRNA in different renal cell types. Further study is needed to understand the mechanism of regulation of Ft-H and Ft-L mRNAs in cisplatin-treated renal cells.

In conclusion, we have found a unique effect of cisplatin on the kidney iron homeostasis in an animal model and different renal cells. We detected upregulation of ferritin subunits both at protein and mRNA levels. The increase of the Ft-L protein and mRNA was higher than that of the Ft-H protein and mRNA in HEK-293, HK-2, and 786-O cells. Similarly, the higher expression of Ft-L than that of Ft-H mRNA and protein was detected in the cisplatin-treated rat kidneys. It did not influence the IRE–IRP interaction despite a significant increase in the HO-1 level, presumably increasing the level of catalytic iron. Expressions of IRE-containing transcripts such as TfR1 and DMT1 responsible for iron uptake remained unaltered that potentially helped to continue the iron uptake. At the same time, the basal level of translation of ferritin subunits was not further increased due to the unaltered IRE–IRP interaction as determined by IRE-containing luciferase assay and RNA-EMSA. Otherwise, the iron-induced elevated ferritin could sequester the increased level of the iron pool. We detected cisplatin-induced kidney injury despite an increased level of ferritin subunits in the adopted animal model. Chronic accumulation of cisplatin in the kidneys is well-reported[41,42] and may continuously generate the iron pool due to elevated HO-1 and if not adequately sequester into ferritin may cause chronic iron accumulation and subsequent renal damage after cisplatin treatment. Our observation of Perl's stain-sensitive iron pool and elevation of non-heme iron in the cisplatin-treated rat kidneys (Figure 8E,F) despite an increase in the ferritin

expression also supports the above-mentioned possibility. Considering the earlier report of amelioration of cisplatin-induced nephrotoxicity by supplementation of iron chelator,[28] our observation thus would be useful in understanding iron accumulation and related nephropathy in cisplatin-treated kidney.

4. MATERIALS AND METHODS

4.1. Cell Culture and Chemicals. HEK-293 (human embryonic kidney) cells were maintained in Dulbecco's modified Eagle medium (DMEM; Sigma-Aldrich), HK-2 (human proximal tubular cells) cells were maintained in Dulbecco's modified Eagle medium nutrient mix F-12 (Ham) (1:1) (DMEM F-12, Gibco Life Technologies), and 786-O (renal adenocarcinoma) cells were maintained in RPMI 1640 (Sigma-Aldrich). All media were supplemented with 10% FBS (Cell Clone) and 1% Pen-Strep (Gibco Life Technologies), and cells were maintained in a humidified atmosphere at 37 °C and 5% CO_2 in a sterile incubator. All treatments were given at 60−70% confluence in culture dishes. Cisplatin (Cytoplatin-50) was procured from Cipla Ltd., India. All other reagents and chemicals unless specified were purchased from Sigma-Aldrich.

4.2. Animals. The animals were housed under controlled temperature and light conditions (24 °C, 12 h light and 12h dark cycle). Food and water were provided ad libitum. Healthy male adult Wistar rats (Rattus novergicus) weighing 200−220 g were randomly grouped into two groups, experimental (cisplatin) and control (saline), at the beginning of the experiment. Cisplatin was used with the aim of developing nephropathy. The dose regimen of cisplatin was standardized as 1 mg/kg body weight by intraperitoneal injection twice a week for 8 weeks. Blood was collected from the retro-orbital venous plexus once before the first cisplatin injection and weekly thereafter for the determination of serum creatinine that served as a marker of renal damage. At the end of 8 weeks, animals were euthanized, and after sacrifice, the kidneys were harvested and stored as per experimental needs. All methodological procedures involving rats were performed in conformity with the guidelines of the Committee for the Purpose of Control and Supervision of Experiments on Animals (CPCSEA), Government of India, and were assessed and approved by the Institutional Animal Ethics Committees (IAEC) of the All India Institute of Medical Sciences (26/IAEC-1/2017), New Delhi, India.

4.3. Western Blot Analysis. Harvested cells and tissues were homogenized, and the whole cell lysate was prepared in a buffer containing 25 mmol/L Tris-HCl (pH 7.5), 0.5 mmol/L EDTA, 25 mmol/L sodium chloride, 10 mmol/L sodium fluoride, 1 mmol/L sodium vanadate, 1% Nonidet P-40, and protease inhibitor cocktails (Roche Diagnostics). Protein concentration was determined by the Bradford protein assay using a kit (Bio-Rad Laboratories), and an equal amount of protein (60 μg until mentioned otherwise) from each sample was denatured by boiling for 5 min in Laemmli buffer. Protein samples were separated on SDS−PAGE and transferred to a poly(vinylidene fluoride) (PVDF) membrane. Membranes were first incubated in a blocking buffer (tris-buffered saline (TBS) containing 0.1% Tween-20 and 5% nonfat dry milk) for 1 h followed by incubation with the respective primary antibodies overnight at 4 °C. Details of primary antibodies used are as follows: anti-Ft-H (Cell Signalling Technology), anti-Ft-L (Abcam), anti-TfR1 (Thermo Fischer Scientific), anti-Fpn (Abcam), anti-HO-1(Novus Biologicals), anti-actin (Santa Cruz Biotechnology), anti-IRP-1 (Santa Cruz Biotechnology),

and anti-IRP-2 (Alpha Diagnostics). Blots were then washed three times in 0.1% Tween containing 1× TBS followed by incubation with the corresponding peroxidase-labeled anti-mouse (Sigma-Aldrich) or anti-rabbit (Thermo Fischer Scientific) secondary antibodies for 1 h at room temperature. The signals were visualized by enhanced chemiluminescence. ImageJ software was used for quantification of protein bands relative to the expression of actin.

4.4. Quantitative Reverse Transcription Polymerase Chain Reaction (qRT-PCR). Total RNA was isolated from the harvested cells or kidney tissues using the TRIzol reagent (Ambion, Life Technologies, #15596026) as per the manufacturer's protocol. A total of 2 μg of total RNA was reverse-transcribed using a cDNA synthesis kit (Applied Biosystems), and qRT-PCR was performed to determine the expressions of Ft-H, Ft-L, TfR1, and DMT1. The primer sets used for human cell lines were $β$-actin (F:5′GCA CCA GGG CGT GAT GG 3′; R: 5′TCC CAG TTG GTG ACG ATG C 3′), FtH (F: 5′TAA GAG ACC ACA AGC GAC C 3′; R: 5′CGT CCA AGC ACT GTT GAA G 3′), FtL (F:5′AGC GTC TCC TGA AGA TGC AA 3′; R: 5′CAG CTG GCT TCT TGA TGT CC 3′), DMT1 (F′:GCA GGA AGT TCG AGA AGC CA 3′; R: 5′AGA CTT CAA CCA CCT GCT CG 3′), and TfR1 (F: 5′ACT GGA CAG CAC AGA CTT CAC 3′; R: 5′TTG ATT TTC AAC ATA CAA CGC AAG A 3′). The primer sets for the kidney tissue of Wistar rats were $β$-actin (F: 5′GCA GGA GTA CGA TGA GTC CG 3′; R: 5′TCA GTA ACA GTC CGC CTA G 3′), FtH (F:5′TGA CCA CGT GAC CAA CTT AC 3′; R:5′AGC TCT CAT CAC CGT GTC C 3′), FtL (F:5′AAC CTC CGT AGG GTG GCA G 3′; R: 5′TAG TCG TGC TTC AGA GTG AG 3′), DMT1 (5′: CTT CCC TCC CAC ATT CCA CC 3′; R: 5′CCT GTG AAG GCC CAG AGT TT 3′), and TfR1 (F: 5′GGC GGA CAA GTC AGA AAA CG 3′; R:5′TCT GAG ATC CAG CCT CAC GA 3′). Expression levels were normalized to the housekeeping gene $β$-actin. PCR was monitored in real time using the Universal SYBR-Green Master (Thermo Fischer Scientific) according to the manufacturer's instructions on a CFX96 Touch real-time PCR detection system (Bio-Rad). Fluorescence curves were analyzed, and automated calculation was carried out by the second-derivative maximum method to give 2^{-ddct} values.

4.5. Determination of the Labile Iron Pool (LIP). The labile iron pool (LIP) was detected using the fluorescence probe calcein-AM.[39] HEK-293 and HK-2 cells were grown on cover slips in 6-well plates and treated with cisplatin. One hour prior to completion of the treatment, media were replaced and loaded with calcein-AM (working concentration: 1 nM in serum-free media) and incubated at 37 °C in the dark. Then, the cells were washed with 1× PBS twice and fixed with 4% formaldehyde (v/v) in 1× PBS for 15 min at room temperature. The fluorescence was monitored at an excitation of 488 nm and an emission of 538 nm using a fluorescence microscope (Carl Zeiss AxioVision).

The LIP level was also estimated as described earlier.[39,40] The cells were grown in 96-well plates and treated with cisplatin after transfecting with the control or Ft-H/Ft-L siRNA. After treatment, the cells were washed with 1×PBS and incubated with 1 μM calcein-AM (Sigma-Aldrich) for 30 min at 37 °C. Then, the cells were washed again with 1× PBS and 100 μL of 145 mM NaCl, pH 7.2; 20 mM HEPES was added. Fluorescence was monitored at an excitation of 488 nm and an emission of 538 nm using a Fluroskan Ascent FL (Thermo Fischer Scientific). The quenching of calcein by the LIP was assessed by the addition of 100 μM pyridoxal hydrazine (PIH) (Santa Cruz Biotechnology).

4.6. Preparation of the Cytosolic Extract. The cytosolic extract was prepared as described earlier.[39,40] In brief, the cells were harvested in ice-cold 1× PBS after the treatment by centrifuging at 1000g for 5 min at 4 °C. Pellets were resuspended in lysis buffer containing 50 mM Tris-Cl (pH-7.5), 50 mM NaCl, 1 mM phenylmethylsulfonylfluoride (PMSF), 0.5 mM DTT, and 1× protease inhibitor cocktail (Roche Diagnostics). The samples were subjected to multiple freeze−thaw cycles and passed through a 30-gauge needle 10−12 times. The mixture obtained was spun at 40,000g for 30 min to harvest the supernatant.

4.7. Cytosolic Aconitase Assay. Cytosolic aconitase assay was performed as described earlier.[39,43] Cytosolic extracts (50 μg) from untreated and cisplatin (0−50 μM)- and ferric ammonium citrate (FAC, 10 μM)-treated cells were added to 0.2 mM cis-aconitate in 100 mM Tris-Cl (pH 7.4), 100 mM NaCl, and 0.02% BSA to perform aconitase assay, and disappearance of cis-aconitate followed at 25 °C at 240 nm.

4.8. Constructions of Vectors. The Ft-H 5′UTR and Ft-L 5′UTR were cloned between HindIII and NcoI restriction sites upstream of the pGL3 control vector as described previously.[43] An Ft-H IRE-containing pcDNA3 plasmid for in vitro transcription was prepared as reported earlier.[43]

4.9. In Vitro Transcription and RNA-Gel-Shift Assay. The pcDNA3 plasmid containing the Ft-H IRE was linearized using BglII and XbaI and transcribed using an in vitro transcription kit (Roche Diagnostics). The cytosolic extract (10 μg) was incubated with (^{32}P) UTP-labeled IRE of the Ft-H 5′UTR in 10 mM Tris-Cl (pH 7.6), 5 mM MgCl$_2$, 15 mM KCl, 0.1 mM DTT, 10 units of RNasin, and 0.2 mg/mL yeast tRNA in a volume of 20 μL to allow the RNA−protein (IRE−IRP) interaction.[39,40] After 15 min of incubation in ice, the mixture was incubated with 1 unit of RNase T1 (10 min) followed by 5 mg/mL heparin (10 min). RNA−protein complexes were then resolved on 5% nondenaturing polyacrylamide gel in 0.5× Tris-borate-EDTA buffer (pH-8) at 4 °C. The gel was dried and subjected to autoradiography.

4.10. Silencing of Ft-H and Ft-L. Silencing of Ft-H and Ft-L in HK-2 and HEK-293 cells was carried out by transfecting siRNAs specific for Ft-H (Sigma Aldrich, SA-SI_HS01_00112824), Ft-L (Sigma Aldrich, SA-SI_HS02_0030196,) and control siRNA (Santa Cruz Biotechnology, sc37007). Transfection was carried out using Lipofectamine-2000 (Thermo Fishcer Scientific) as per the manufacturer's protocol. The efficacy of silencing was verified by immunoblot analysis.

4.11. Flow Cytometry. Cell death assay was performed using a kit as per the manufacturer's instruction (Molecular Probes, Invitrogen, Cat #V13241). Briefly, HK-2 cells were treated with cisplatin after appropriate transfection by siRNAs and harvested by mild trypsinization, washed with 1× PBS, and resuspended in 100 μL of 1× Annexin V binding buffer (1×10^6 cells/ml). The cells were then incubated with Alexa Fluor 488 Annexin and propidium iodide at room temperature 15 min. After that, 400 μL of 1× Annexin V binding buffer was added, and the cells were kept on ice until analysis. The samples were analyzed by flow cytometry (FACSCanto™ II, BD Biosciences) using FACSDiva software and FlowJo software (Tree Star). Average survival (%) from three different experiments was plotted as a bar graph.

4.12. Dual-Luciferase Reporter Assay. The cells were transfected with the pGL3 luciferase reporter vector (Promega, E1741) containing the 5′UTR of Ft-H/ Ft-L upstream of the luciferase gene along with the thymidine kinase promoter containing the Renilla luciferase reporter plasmid (pRL-TK, Promega, E2231). Cells were kept in the transfection cocktail containing both reporter vectors and Turbofect (Thermo Fischer Scientific, R0531) in serum-free DMEM. The transfection cocktail was replaced after 6 h with fresh media and left overnight for recovery. Then, the cells were incubated with cisplatin (0−50 μM) or ferric ammonium citrate (FAC, 10 μM) (as a positive control). Cells were lysed after 16 h, and luminescence was measured as per the protocol of the Dual-Luciferase Reporter (DLR) Assay System (Promega, E1910). Results were normalized to Renilla luminescence.

4.13. Histopathology of the Kidney Tissue. Formalin-fixed paraffin-embedded kidney tissues were cut into 5 μM sections with periodic acid-Schiff (PAS) reagent and Masson's trichrome (MT) staining. Tubular damage was scored on a scale of 0−5, 0 indicating no tubular damage; 1 indicating <10% damage; 2 indicating 10−25% damage; 3 indicating 25−50% damage; 4 indicating 50−75% damage; and 5 indicating >75% damage.[44] The tubulointerstitial fibrosis score was calculated from MT-stained sections varied from 0 to 3; 0 indicating no evidence of fibrosis; 1 indicating <25% fibrosis; 2 indicating 25−50% fibrosis; and 3 indicating >50% fibrosis.[44] For Perl's Prussian Blue staining, a fresh mixture containing an equal proportion of 20% hydrochloric acid and 10% potassium ferrocyanide was used, and nuclear fast red dye was used as a counterstain.[45] Slides containing the stained sections were then washed in water, air-dried, and mounted in DPX. Non-overlapping microscopic fields were captured using a Nikon Eclipse E600.

4.14. Estimation of Non-heme Iron. Non-heme iron estimation in tissue was performed as described earlier.[46] Briefly, the tissue (50 mg) was homogenized in 1:10 (w/v) water. The tissue homogenate (100 μL) was transferred to a fresh microcentrifuge tube and mixed with protein precipitation solution (1N HCl and 10% TCA in water). The mixture was vortexed and kept at 95 °C in a heating block for 1 h. Tubes were cooled at room temperature for 5 min and vortexed again followed by centrifugation for 2 min at 10,000g. A clear supernatant was transferred to a 96-well flat-bottom plate and mixed with 20 μL of chromogen solution (0.508 mmol/L ferrozine, 1.5 mol/L sodium acetate, and 0.1% thioglycolic acid (TGA) in water). Blanks were prepared by adding 50 μL of water and 50 μL of protein precipitation solution mixed with 20 μL of chromogen solution. Serial dilutions of ferrous ammonium sulfate solution were processed similarly like the tissue homogenate to plot the standard curve. The samples, blank, and standards were incubated at room temperature for 30 min before calculating absorbance at 560 nm. Final results were calculated as μg of iron per gram wet tissue weight.

4.15. Estimation of Serum Ferritin and Serum Creatinine. Quantitative detection of ferritin in serum samples collected from animals was done using a Sandwich ELISA kit (E-EL-R3018, ElabScience Biotechnology) specific for rat ferritin as per the protocol provided in the kit. Similarly, creatinine was estimated in serum samples collected from animals using a kit (Cat # ref No. CRS 100, Medsource Ozone Biomedicals Pvt. Ltd.) as per the protocol provided in the kit.

4.16. Statistics. Quantitative and qualitative data represent at least three independent experiments. The bar and line graphs represent the mean, and the error bar represents the standard deviation unless mentioned otherwise. Statistical analysis was done using the "Data Analysis" tool of MS Excel version 15.26

(160910). Student's *t*-test and ANOVA were used as applicable to calculate the p value. We used $p \leq 0.05$ as a statistically significant difference.

ASSOCIATED CONTENT

Supporting Information

The Supporting Information is available free of charge at https://pubs.acs.org/doi/10.1021/acsomega.1c06716.

Expression of IRP1 in different cell types; cisplatin promotes ROS generation in HEK-293 cells; and serum ferritin in cisplatin-treated rats (PDF)

AUTHOR INFORMATION

Corresponding Authors

Amit K. Dinda − *Department of Pathology, All India Institute of Medical Sciences, New Delhi 110029, India;* ⊙ orcid.org/0000-0003-0472-8966; Email: dindaaiims@gmail.com

Chinmay K. Mukhopadhyay − *Special Centre for Molecular Medicine, Jawaharlal Nehru University, New Delhi 110067, India;* ⊙ orcid.org/0000-0001-7094-3088; Email: ckm2300@mail.jnu.ac.in

Author

Ayushi Aggarwal − *Department of Pathology, All India Institute of Medical Sciences, New Delhi 110029, India*

Complete contact information is available at:
https://pubs.acs.org/10.1021/acsomega.1c06716

Notes

The authors declare no competing financial interest.
The funding agency has no role in conducting the research, study design, collection, analysis, and interpretation of data or submission of the article.

ACKNOWLEDGMENTS

ABBREVIATIONS

DCF, dichlorodihydrofluorescein; DMT-1, divalent Metal Transporter-1; DTT, dithiothreitol; EMSA, electrophoretic mobility shift assay; FAC, ferric ammonium citrate; Ft-H, ferritin-H; Ft-L, ferritin-L; HO-1, heme oxygenase-1; IRP, iron regulatory protein; LIP, labile iron pool; PMSF, phenyl-methysulfonylfluoride; ROS, reactive oxygen species; siRNA, small interfering RNA; TBS, tris-buffered saline; TfR1, transferrin Receptor-1; TGA, thioglycolic acid; UTR, untranslated region

REFERENCES

(1) Hartmann, J. T.; Fels, L. M.; Knop, S.; Stolt, H.; Kanz, L.; Bokemeyer, C. A randomized trial comparing the nephrotoxicity of cisplatin/ifosfamide-based combination chemotherapy with or without amifostine in patients with solid tumors. *Invest. New Drugs* **2000**, *18*, 281−289.

(2) Hartmann, J. T.; Lipp, H. P. Toxicity of platinum compounds. *Expert Opin. Pharmacother.* **2003**, *4*, 889−901.

(3) Arany, I.; Safirstein, R. L. Cisplatin nephrotoxicity. *Semin. Nephrol.* **2003**, *23*, 460−464.

(4) Sastry, J.; Kellie, S. J. Severe Neurotoxicity, Ototoxicity And Nephrotoxicity Following High-Dose Cisplatin And Amifostine. *Pediatr. Hematol. Oncol.* **2005**, *22*, 441−445.

(5) Ishida, S.; Lee, J.; Thiele, D. J.; Herskowitz, I. Uptake of the anticancer drug cisplatin mediated by the copper transporter Ctr1 in yeast and mammals. *Proc. Natl. Acad. Sci.* **2002**, *99*, 14298−14302.

(6) Ludwig, T.; Riethmüller, C.; Gekle, M.; Schwerdt, G.; Oberleithner, H. Nephrotoxicity of platinum complexes is related to basolateral organic cation transport. *Kidney Int.* **2004**, *66*, 196−202.

(7) Ciarimboli, G.; Ludwig, T.; Lang, D.; Pavenstädt, H.; Koepsell, H.; Piechota, H.-J.; Haier, J.; Jaehde, U.; Zisowsky, J.; Schatter, E. Cisplatin Nephrotoxicity Is Critically Mediated via the Human Organic Cation Transporter 2. *Am. J. Pathol.* **2005**, *167*, 1477−1484.

(8) Miller, R. P.; Tadagavadi, R. K.; Ramesh, G.; Reeves, W. B. Mechanisms of Cisplatin Nephrotoxicity. *Toxins* **2010**, *2*, 2490−2518.

(9) Pascoe, J. M.; Roberts, J. J. Interactions between mammalian cell DNA and inorganic platinum compounds—II. *Biochem. Pharmacol.* **1974**, *23*, 1359−1365.

(10) Cullen, K. J.; Yang, Z.; Schumaker, L.; Guo, Z. Mitochondria as a critical target of the chemotheraputic agent cisplatin in head and neck cancer. *J. Bioenerg. Biomembr.* **2007**, *39*, 43−50.

(11) Ramesh, G.; Reeves, W. B. TNF-α mediates chemokine and cytokine expression and renal injury in cisplatin nephrotoxicity. *J. Clin. Invest.* **2002**, *110*, 835−842.

(12) Baliga, R.; Zhang, Z.; Baliga, M.; Ueda, N.; Shah, S. V. In vitro and in vivo evidence suggesting a role for iron in cisplatin-induced nephrotoxicity. *Kidney Int.* **1998**, *53*, 394−401.

(13) Shah, S. V.; Rajapurkar, M. M.; Baliga, R. The Role of Catalytic Iron in Acute Kidney Injury. *Clin. J. Am. Soc. Nephrol.* **2011**, *6*, 2329−2331.

(14) Scindia, Y.; Leeds, M. J.; Swaminathan, M. S. Iron Homeostasis in Healthy Kidney and its Role in Acute Kidney Injury. *Semin. Nephrol.* **2019**, *39*, 76−84.

(15) Smith, C. P.; Thevenod, F. Iron transport and the kidney. *Biochim. Biophys. Acta, Gen. Subj.* **2009**, *1790*, 724−730.

(16) Zhang, D.; Meyron-Holtz, E.; Rouault, T. A. Renal Iron Metabolism: Transferrin Iron Delivery and the Role of Iron Regulatory Proteins. *J. Am. Soc. Nephrol.* **2007**, *18*, 401−406.

(17) Fujishiro, H.; Yano, Y.; Takada, Y.; Tanihara, M.; Himeno, S. Roles of ZIP8, ZIP14, and DMT1 in transport of cadmium and manganese in mouse kidney proximal tubule cells. *Metallomics* **2012**, *4*, 700−708.

(18) Li, J. Y.; Paragas, N.; Ned, R. M.; Qiu, A.; Viltard, M.; Leete, T.; Drexler, I. R.; Chen, X.; Sanna-Cherchi, S.; Mohammed, F.; Williams, D.; Lin, C. S.; Schmidt-Ott, K. M.; Andrews, N. C.; Barasch, J. Scara5 Is a Ferritin Receptor Mediating Non-Transferrin Iron Delivery. *Dev. Cell* **2009**, *16*, 35−46.

(19) Mendes-Jorge, L.; Ramos, D.; Valença, A.; López-Luppo, M.; Pires, V. M. R.; Catita, J.; Nacher, V.; Navarro, M.; Carretero, A.; Rodriguez-Baeza, A.; Ruberte, J. Correction: L-Ferritin Binding to Scara5: A New Iron Traffic Pathway Potentially Implicated in Retinopathy. *PLoS One* **2017**, *12*, No. e180288.

(20) Canonne-Hergaux, F.; Gros, P. Expression of the iron transporter DMT1 in kidney from normal and anemic mk mice. *Kidney Int.* **2002**, *62*, 147−156.

(21) Gálvez-Peralta, M.; Wang, Z.; Bao, S.; Knoell, D. L.; Nebert, D. W. Tissue-Specific Induction of Mouse ZIP8 and ZIP14 Divalent Cation/Bicarbonate Symporters by, and Cytokine Response to, Inflammatory Signals. *Int. J. Toxicol.* **2014**, *33*, 246−258.

(22) Levi, S.; Yewdall, S. J.; Harrison, P. M.; Santambrogio, P.; Cozzi, A.; Rovida, E.; Albertini, A.; Arosio, P. Evidence of H- and L-chains have co-operative roles in the iron-uptake mechanism of human ferritin. *Biochem. J.* **1992**, *288*, 591−596.

(23) Abboud, S.; Haile, D. A Novel Mammalian Iron-regulated Protein Involved in Intracellular Iron Metabolism. *J. Biol. Chem.* **2000**, *275*, 19906−19912.

(24) Hentze, M. W.; Muckenthaler, M.; Galy, B.; Camaschella, C. Two to Tango: Regulation of Mammalian Iron Metabolism. *Cell* **2010**, *142*, 24−38.

(25) Rouault, T. A. The role of iron regulatory proteins in mammalian iron homeostasis and disease. *Nat. Chem. Biol.* **2006**, *2*, 406−414.

(26) Nath, K. A.; Balla, G.; Vercellotti, G. M.; Balla, J.; Jacob, H. S.; Levitt, M. D.; Rosenberg, M. E. Induction of heme oxygenase is a rapid, protective response in rhabdomyolysis in the rat. *J. Clin. Invest.* **1992**, *90*, 267−270.

(27) Stocker, R. Antioxidant Activities of Bile Pigments. *Antioxid. Redox Signaling* **2004**, *6*, 841−849.

(28) Agarwal, A.; Balla, J.; Alam, J.; Croatt, A. J.; Nath, K. A. Induction of heme oxygenase in toxic renal injury: A protective role in cisplatin nephrotoxicity in the rat. *Kidney Int.* **1995**, *48*, 1298−1307.

(29) Miyazawa, M.; Bogdan, A. R.; Tsuji, Y. Perturbation of Iron Metabolism by Cisplatin through Inhibition of Iron Regulatory Protein 2. *Cell Chem. Biol.* **2019**, *26*, 85−97.

(30) Zarjou, A.; Bolisetty, S.; Joseph, R.; Traylor, A.; Apostolov, E. O.; Arosio, P.; Balla, J.; Verlander, J.; Darshan, D.; Kuhn, L. C.; Agarwal, A. Proximal tubule H-ferritin mediates iron trafficking in acute kidney injury. *J. Clin. Invest.* **2013**, *123*, 4423−4434.

(31) Hausmann, A.; Lee, J.; Pantopoulos, K. K. Redox control of iron regulatory protein 2 stability. *FEBS Lett.* **2011**, *585*, 687−692.

(32) Ma, Y.; Abbate, V.; Hider, R. Iron-sensitive fluorescent probes: monitoring intracellular iron pools. *Metallomics* **2015**, *7*, 212−222.

(33) Kakhlon, O.; Cabantchik, Z. The labile iron pool: character-ization, measurement, and participation in cellular processes. *Free Radical Biol. Med.* **2002**, *33*, 1037−1046.

(34) Santos, N. A. G.; Catão, C.; Martins, N.; Curti, C.; Bianchi, M.; Santos, A. Cisplatin-induced nephrotoxicity is associated with oxidative stress, redox state unbalance, impairment of energetic metabolism and apoptosis in rat kidney mitochondria. *Arch. Toxicol.* **2007**, *81*, 495−504.

(35) Deng, Z.; Manz, D. H.; Torti, S. V.; Torti, F. M. Iron-responsive element-binding protein 2 plays an essential role in regulating prostate cancer cell growth. *Oncotarget* **2017**, *8*, 82231−82243.

(36) Wang, W.; Deng, Z.; Hatcher, H.; Miller, L. D.; Di, X.; Tesfay, L.; Sui, G.; D'Agotino, R. B.; Torti, F. M.; Torti, S. V. IRP2 Regulates Breast Tumor Growth. *Cancer Res.* **2014**, *74*, 497−507.

(37) Maffettone, C.; Chen, G.; Drozdov, I.; Ouzounis, C.; Pantopoulos, K. Tumorigenic Properties of Iron Regulatory Protein 2 (IRP2) Mediated by Its Specific 73-Amino Acids Insert. *PLoS One* **2010**, *5*, No. e10163.

(38) Das, N. K.; Sandhya, S.; Vivek, V. G.; Kumar, R.; Singh, A. K.; Bal, S. K.; Kumari, S.; Mukhopadhyay, C. K. *Leishmania donovani* inhibits ferroportin translation by modulating FBXL5-IRP2 axis for its growth within host macrophages. *Cell. Microbiol.* **2018**, *20*, No. e12834.

(39) Gupta, P.; Singh, P.; Pandey, H.; Seth, P.; Mukhopadhyay, C. K. Phosphoinositide-3-kinase inhibition elevates ferritin level resulting depletion of labile iron pool and blocking of glioma cell proliferation. *Biochim. Biophys. Acta, Gen. Subj.* **2019**, *1863*, 547−564.

(40) Tapryal, N.; Vivek, G. V.; Mukhopadhyay, C. K. Catecholamine Stress Hormones Regulate Cellular Iron Homeostasis by a Posttran-scriptional Mechanism Mediated by Iron Regulatory Protein. *J. Biol. Chem.* **2015**, *290*, 7634−7646.

(41) Pabla, N.; Dong, Z. Cisplatin nephrotoxicity: mechanisms and renoprotective strategies. *Kidney Int.* **2008**, *73*, 994−1007.

(42) dos Santos, N. A. G.; Rodrigues, M. A. C.; Martins, N. M.; dos Santos, A. C. Cisplatin induced nephrotoxicity and targets of nephroprotection: an update. *Arch. Toxicol.* **2012**, *86*, 1233−1250.

(43) Dev, S.; Kumari, S.; Singh, N.; Bal, S. K.; Seth, P.; Mukhopadhyay, C. K. Role of extracellular Hydrogen peroxide in regulation of iron homeostasis genes in neuronal cells: Implication in iron accumulation. *Free Radical Biol. Med.* **2015**, *86*, 78−89.

(44) Souza, A. C. P.; Tsuji, T.; Baranova, I. N.; Bocharov, A. V.; Wilkins, K. J.; Street, J. M.; Alvarev-Prats, A.; Hu, X.; Eggerman, T.; Yuen, P. S.; Star, R. A. TLR 4 mutant mice are protected from renal fibrosis and chronic kidney disease progression. *Physiol. Rep.* **2015**, *3*, No. e12558.

(45) Sun, Y.; Gou, G. J.; Dong, L. E. Intracellular Trafficking Characteristics for Magnetic Layered Double Hydroxide/DNA Hybrids to Human Gastric Cancer Cells. *Appl. Mech. Mater.* **2013**, *320*, 529−532.

(46) Rebouche, C. J.; Wilcox, C. L.; Widness, J. A. Microanalysis of non-heme iron in animal tissues. *J. Biochem. Biophys. Methods* **2004**, *58*, 239−251.